Cell Biology. In the article "Cell locomotion and focal adhesions are regulated by substrate flexibility" by Robert J. Pelham, Jr., and Yu-li Wang, which appeared in number 25, December 9, 1997, of *Proc. Natl. Acad. Sci. USA* (**94,** 13661–13665), the authors wish to publish the following corrections to Fig. 1. The *y* axis of Fig. 1*B* should be labeled with "0" at the origin and should cover a range of 0–80. The numbers placed along the *y* axis were misaligned with respect to the scale on the graph. Also, the unit should have been "10^3 N/m^2" instead of "N/m^2" as originally indicated in the legend. The corrected figure and its legend are shown below.

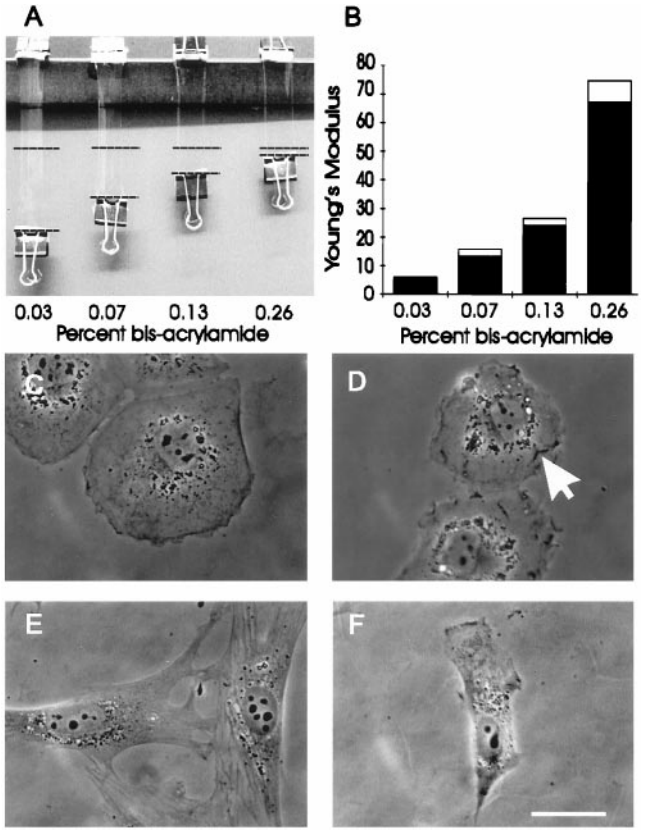

FIG. 1. Mechanical characteristics of polyacrylamide substrates and effects on cell morphology. (*A* and *B*) identically sized strips of polyacrylamide with various acrylamide/bis-acrylamide ratios were fixed at one end and stretched at the other end with a downward force of 0.103 N. The dashed lines represent the amount of stretching caused by applied weight (*A*). The extent of stretching was then used for the calculation of Young's modulus, expressed as 10^3 N/m^2 (*B*). (*C–F*) Phase morphology of NRK (*C* and *D*) or 3T3 (*E* and *F*) cells plated on substrates containing 0.26% bis- (*C* and *E*) or 0.03% bis-acrylamide (*D* and *F*). NRK cells on the more flexible substrate are less well spread and contain irregular ruffles on the ventral surface (*D*, arrow), as determined by optical sectioning at a high magnification. Similarly, 3T3 cells on the substrate of high flexibility are typically less well spread and with a polarized morphology (*F*). Bar = 10 μm.

Physiology. In the article "Molecular cloning and expression of a cyclic AMP-activated chloride conductance regulator: A novel ATP-binding cassette transporter" by Marcel A. van Kuijck, Rémon A. M. H. van Aubel, Andreas E. Busch, Florian Lang, Frans G. M. Russel, René J. M. Bindels, Carel H. van Os, and Peter M. T. Deen, which appeared in number 11, May 28, 1996, of *Proc. Natl. Acad. Sci. USA* (**93,** 5401–5406), the authors wish to note the following. "The experiments involving expression in *Xenopus* oocytes cannot be reproduced. Therefore, the conclusion that this cDNA encodes a cAMP-regulated chloride transporter is incorrect. The correct functional activity of the cloned transporter has now been assessed by expression in insect Sf9 cells and reported in ref 1. The cloned cDNA turned out to be the rabbit homologue of the rat and human canalicular multispecific organic anion transporter, cMOAT, which is identical to the multidrug resistance-associated protein MRP2, as published in ref. 2. The sequence information is now available in GenBank (accession no. Z49144) under rabbit mrp2 gene for multidrug resistance-associated protein 2."

1. van Aubel, R., van Kuijck, M., Koenderink, J., Deen, P., van Os, C. & Russel, F. (1998) *Mol. Pharmacol.* **53,** 1062–1067.
2. van Kuijck, M., Kool, M., Merkx, G., van Kessel, A. D., Bindels, R., Deen, P. & van Os, C. (1997) *Cytogenet. Cell Genet.* **77,** 285–287.

Psychology. In the article "Social stress and the reactivation of latent herpes simplex virus type 1" by David A. Padgett, John F. Sheridan, Julianne Dorne, Gary G. Berntson, Jessica Candelora, and Ronald Glaser, which appeared in number 12, June 9, 1998, of *Proc. Natl. Acad. Sci. USA* (**95,** 7231–7235), the following correction should be noted. The *x* axis in Fig. 2 should read "Days of social reorganization" rather than "Days of restraint." A corrected figure and its legend are shown below.

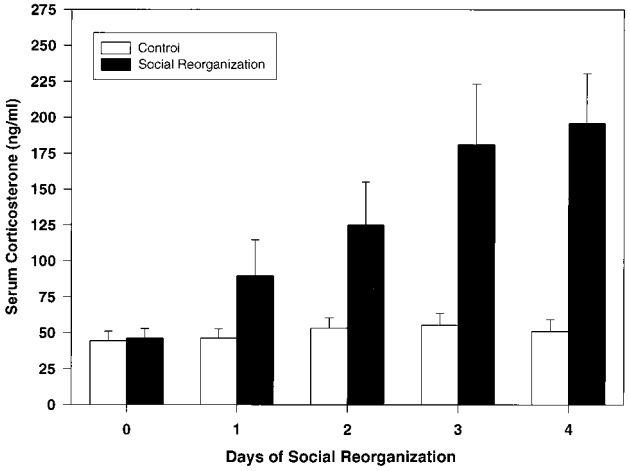

FIG. 2. Influence of social reorganization on serum corticosterone. Data represent 10 a.m. serum corticosterone as measured by RIA. Baseline samples were obtained 2 days before initiation of any experimental manipulations. For social reorganization, dominant animals were identified and placed in new cages at 6 p.m. the evening before blood sampling. n = 5 animals per group at each time point.

Genetics. In the article, "A member of a family of sulfate-activating enzymes causes murine brachymorphism," by Kiyoto Kurima, Matthew L. Warman, Srinivasan Krishnan, Miriam Domowicz, Richard C. Krueger, Jr., Andrea Deyrup, and Nancy B. Schwartz, which appeared in number 15, July 21, 1998, of *Proc. Natl. Acad. Sci. USA* (**95,** 8681–8685), the following correction should be noted. An early version of Fig. 2 containing several errors was printed. The corrected figure and its legend are reproduced below. This version contains sequence data identical to that which was deposited in the GenBank database (accession no. AF052453) on March 4, 1998.

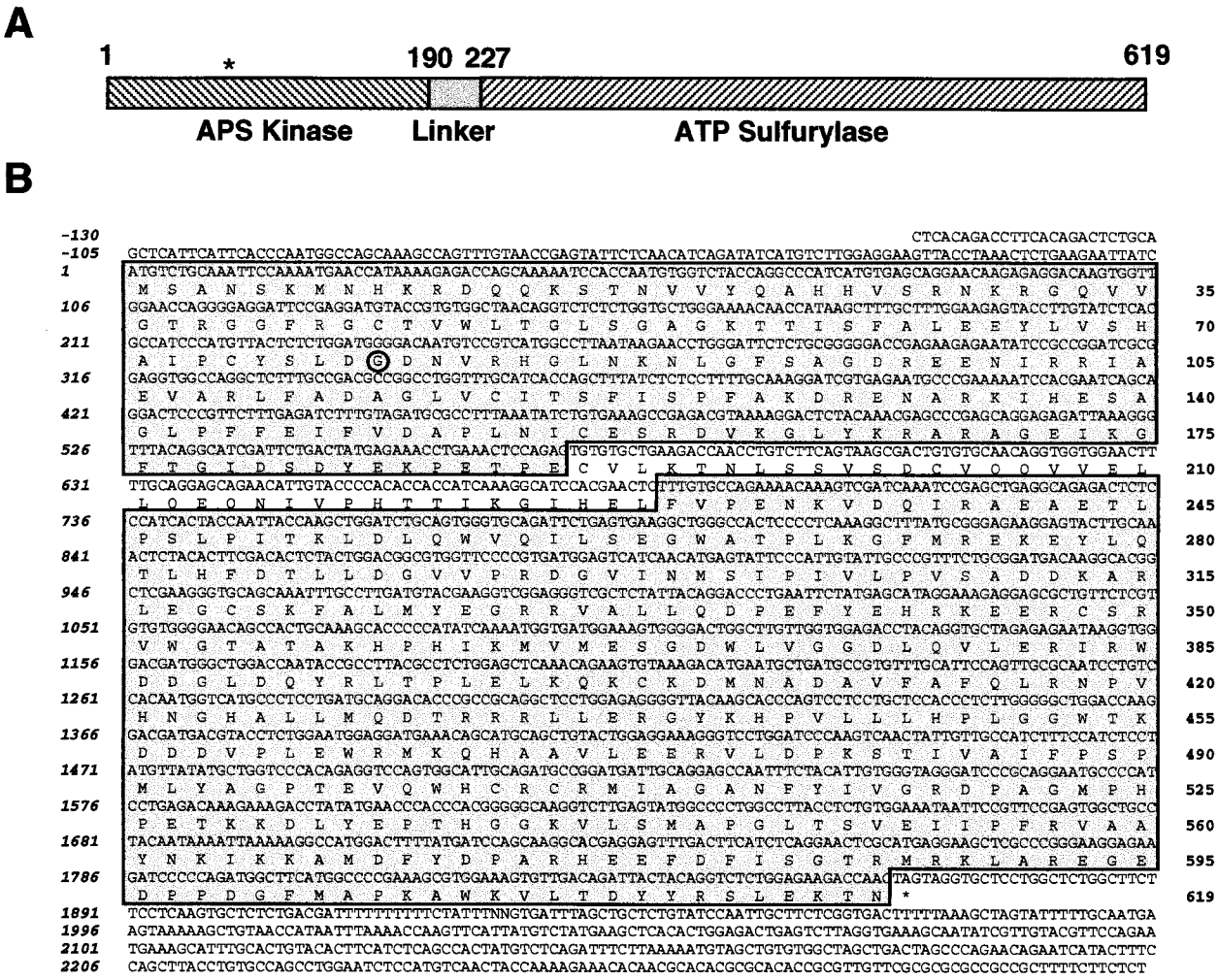

FIG. 2. Sequence of *SK2*. (*A*) Schematic diagram of ATP sulfurylase/APS kinase. Approximate location of the mutation in *bm SK2* is indicated by ∗. (*B*) The cDNA sequence and its deduced amino acid sequence are shown. The mutation found in *bm SK2* is circled.

Proc. Natl. Acad. Sci. USA
Vol. 95, pp. 8681–8685, July 1998
Genetics

A member of a family of sulfate-activating enzymes causes murine brachymorphism

KIYOTO KURIMA*, MATTHEW L. WARMAN†, SRINIVASAN KRISHNAN*, MIRIAM DOMOWICZ*, RICHARD C. KRUEGER, JR.*, ANDREA DEYRUP*, AND NANCY B. SCHWARTZ*‡

*Departments of Pediatrics and Biochemistry and Molecular Biology, University of Chicago, MC 5058, 5825 S. Maryland Avenue, Chicago, IL 60637; and †Departments of Genetics and Pediatrics, Case Western Reserve University School of Medicine and Center for Human Genetics, University Hospitals of Cleveland, 10900 Euclid Avenue, Cleveland, OH 44106

Communicated by Elizabeth D. Hay, Harvard Medical School, Boston, MA, May 22, 1998 (received for review April 4, 1998)

ABSTRACT **Sulfation is critical to the function of a wide variety of biomolecules. This common modification requires the enzymatic synthesis of an activated sulfate donor, phosphoadenosine-phosphosulfate (PAPS). In higher organisms PAPS synthesis is catalyzed by a bifunctional sulfurylase kinase (SK) polypeptide having both ATP-sulfurylase and adenosine-phosphosulfate kinase activities. We report the identification of a gene family encoding murine SK proteins with these two activities. A family member, *SK2*, colocalizes with the locus for the autosomal recessive murine phenotype brachymorphism. Brachymorphic mice have normal lifespans, but abnormal hepatic detoxification, bleeding times, and postnatal growth, the latter being attributed to undersulfation of cartilage proteoglycan. A missense mutation in the *SK2* coding sequence of *bm* mice that alters a highly conserved amino acid residue destroys adenosine-phosphosulfate kinase activity and therefore the ability of SK2 to synthesize PAPS. We conclude that a family of *SK* genes are responsible for sulfate activation in mammals, that a mutation in *SK2* causes murine brachymorphism, and that members of this gene family have nonredundant, tissue-specific roles.**

Sulfation is a necessary modification of proteins, carbohydrates, and lipids. One of the most prominent roles of sulfation in vertebrates is the posttranslational modification of glycosaminoglycans, the repeating disaccharide chains that are covalently linked to protein cores to constitute the family of proteoglycans. Sulfation requires active transport of sulfate into the cell, conversion into the "active" high energy form of phosphoadenosine-phosphosulfate (PAPS), translocation of PAPS across the golgi membrane, and transfer of sulfate from PAPS, via a multitude of sulfotransferases, to the recipient biomolecules (1). The sulfate activation pathway consists of two activities, ATP-sulfurylase (EC 2.7.7.4), which catalyzes synthesis of adenosine-phosphosulfate (APS) from ATP and SO_4^{-2}, and APS kinase (EC 2.7.1.25), which phosphorylates APS in the presence of another molecule of ATP to form PAPS. In simpler organisms these activities are catalyzed by separate enzymes (2–5). In contrast, when these two sulfate-activating activities were purified from rat chondrosarcoma they were found to exist as a bifunctional enzyme (6, 7), which uses a channeling mechanism to transfer the intermediate APS efficiently from the sulfurylase to the kinase active site (8–10). Subsequently, a mouse cDNA encoding a fused ATP-sulfurylase/APS kinase was isolated. This mammalian PAPS synthetase (referred to as SK1) is a bifunctional polypeptide that catalyzes both ATP-sulfurylase and APS-kinase reactions (11).

Murine brachymorphism is characterized by dome-shaped skull, short thick tail, and shortened but not widened limbs (12, 13) and has been attributed to a defective PAPS synthesis pathway (14–17). The phenotype is inherited as an autosomal recessive, and *bm* homozygotes breed normally, have life spans comparable to wild-type mice, and are about the same size as normals at birth. The difference in size becomes apparent over the first 4 weeks of life, resulting in a 50% reduction in limb length and a 25% reduction in axial skeletal size (Fig. 1). The effect on growth is concomitant with a progressive reduction in size of the columnar and hypertrophic zones in the epiphyseal growth plates. Histological and ultrastructual studies suggest a defective cartilage matrix that contains normal collagen fibrils, but proteoglycan aggregate granules that are smaller than normal and present in reduced numbers, particularly in the growth plate (18). Biochemical analysis showed that brachymorphic cartilage contains normal levels of glycosaminoglycans but with disaccharides that are significantly undersulfated. The reduced incorporation of sulfate in brachymorphic cartilage is associated with limited PAPS availability because of a reduction predominantly in APS-kinase activity (14–17). Genetic linkage studies localized the *bm* gene on chromosome 19 (12, 19). However, the precise gene responsible for brachymorphism has not been identified.

Here we report the isolation of an additional member of the PAPS synthetase family, *SK2*, and the chromosomal localization of both *SK1* and *SK2* genes. *SK2* is mapped on chromosome 19 and is tightly linked with the marker for *bm* locus (19). Sequence analysis of a *bm SK2* cDNA revealed a missense mutation that results in a glycine-to-arginine substitution at a highly conserved portion of the APS-kinase domain, and bacterially expressed *bm* SK2 fails to catalyze the APS-kinase reaction and to synthesize PAPS. These findings indicate that the mutation in the *SK2* gene is responsible for murine brachymorphism.

MATERIALS AND METHODS

Identification and Cloning of *SK2*. The deduced amino acid sequence of *SK1* (GenBank accession no. U34883) was used as a BLAST query sequence against the expressed sequence tag (EST) database maintained by the National Center for Biotechnology Information at the National Library of Medicine. Nucleotide sequences from several EST clones suspected to contain *SK2* cDNA initially were used to generate oligonucleotide primers. The 5′-end of a cDNA sequence subsequently was obtained by the 5′-inverse PCR method (20). Reverse

The publication costs of this article were defrayed in part by page charge payment. This article must therefore be hereby marked "*advertisement*" in accordance with 18 U.S.C. §1734 solely to indicate this fact.

Abbreviations: SK, sulfurylase kinase; PAPS, phosphoadenosine-phosphosulfate; APS, adenosine-phosphosulfate; EST, expressed sequence tag.

Data deposition: The *SK2* cDNA sequence reported in this paper has been deposited in the GenBank database (accession no. AF052453).

‡To whom reprint requests should be addressed. e-mail: n-schwartz@uchicago.edu.

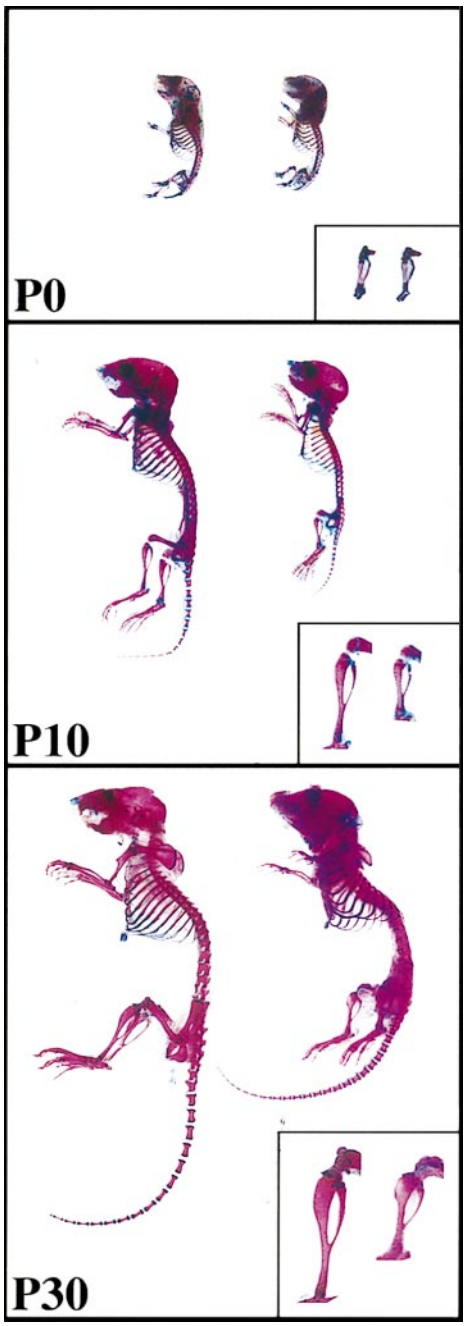

FIG. 1. Postnatal skeletal development of normal (*Left*) and *bm* (*Right*) mice. Calcified bone and cartilage were differentially stained with Alzarin red and Alcian blue, respectively, at zero (P0), 10 (P10), and 30 (P30) days after birth. (*Insets*) Tibias of normal (*Left*) and *bm* (*Right*) mice. Note the similar size in all of the skeletal elements at P0 and the slower increases in the length of the brachymorphic skeletal elements.

transcription–PCR (RT-PCR) was performed on total RNA extracted from normal and *bm* neonatal livers. The first strand was synthesized by SuperScript II (GIBCO/BRL) using an antisense primer (SK5, 5′-GCAATTGGATACAGAGCAGC-3′) complementary to the 3′-untranslated region of *SK2* mRNA. The complete ORF cDNA was amplified with a 5′-end sense primer containing a *Nde*I site (SK30, 5′-AGAGAGTTCCATATGTCTGCAAATTCCAAAATGAACCATAAAAGAGACCAGC-3′) and a 3′-end antisense primer containing a *Xho*I site (SK31, 5′-GAGAGAGATCTCGAGCTAGTTGGTCTTCTCCAGAGACCTGTAGTAATCTGTCAACAC-3′) using Expand (Boehringer-Mannheim). RT-PCR of the total liver RNA yielded a single band approximately 1.9 kb in length. The fragment was digested with *Nde*I and *Xho*I and cloned into appropriate restriction sites in a bacterial expression vector, pET-15b (Novagen). The nucleotide sequence was determined by the dideoxynucleotide chain termination method using T7 sequenase kit (Amersham). To confirm the *bm SK2* mutation at nucleotide 235, genomic DNA sequence at the nucleotide 235 site from the normal and *bm* mice was determined after amplifying genomic DNA fragments by PCR using a set of two primers flanking the mutation site (SK15, 5′-CAGTAGATCTCGAGTGCGGATATTCTCTTCTCGGTCC-3′; SK26, 5′-CAACAATAAGCTTTCCTTTGGAAGAGTACC-3′).

Northern Blot Analysis. Livers were dissected from neonatal normal and *bm* mice and immediately frozen on dry ice, and total RNA was isolated by using TRIzol (GIBCO/BRL). Fifteen micrograms of total liver RNA was electrophoresed in a 1% agarose-formaldehyde gel and transferred to a Nytran filter. Prehybridization, hybridization with the ^{32}P-labeled 1.9-kb *SK2* cDNA, and washing were performed as previously described (11). The same filter was stripped and rehybridized with a mouse β-actin cDNA probe.

Recombinant Enzyme Assays. An *Escherichia coli* strain, BL21(DE3), was transformed by the heat-shock method with a *SK2* cDNA cloned in pET-15b vector (Novagen). Isopropyl β-D-thiogalactoside (10 mM) was added to an overnight bacterial culture and incubated for an additional 4 hr. The bacterial cell cultures were centrifuged at 9,000 $\times$ *g*, and the pellet was resuspended into IMAC 5 buffer (5 mM imidazole/50 mM Tris, pH 7.9). The protein was purified after cell sonication and gravity His-tag purification (Novagen) and quantitated by the Pierce BCA protein assay method. Purified enzyme was dialysed into phosphate buffer (25 mM NaH_2PO_4-K_2HPO_4, pH 7.8/1 mM DTT/1 mM EDTA) overnight and diluted with phosphate buffer to 20 μg/ml for enzymatic assays. Crude extracts from bacteria carrying the vector without insert and no vector were used as negative controls. The ATP-sulfurylase was assayed in the reverse direction of ATP formation as described (8). Standard ATP-sulfurylase assays contained 50 mM NaH_2PO_4-K_2HPO_4 (pH 7.8), 12 mM $MgCl_2$, 0.5 mM DTT, 5 mM NaF, 0.2 mM $Na_4P_2O_7$ (containing 6.7 mCi of ^{32}P), 0.1 mM APS, and 50 μl of enzyme preparation. APS kinase was assayed as described (10). Standard APS-kinase assay contained 80 nM [^{35}S]APS, 0.5 mM ATP (pH 7.0), 5 mM $MgCl_2$, 10 mM ammonium sulfate, and 12 μl of enzyme, brought up to 25 μl with buffer A (25 mM NaH_2PO_4-K_2HPO_4, pH 7.8/1 mM DTT/1 mM EDTA/10% glycerol). The overall reaction with ATP and SO_4^{2-} as substrates and measuring the production of APS and PAPS was assayed as described (6). The 25-μl standard overall reaction contained 0.4 mM [^{35}S]H_2SO_4, 10 mM ATP, 20 mM $MgCl_2$, 22 mM Tris·HCl (pH 8.0), and 15 μl of enzyme preparation.

Chromosomal Localization. A murine *SK1* PCR product from primer pair SK16 (5′-GGAAACGGCCTGATTTCAGG-3′) and SK21 (5′-CACGCGAAGGCCAGAAACC-3′) was used to amplify a 190-bp intragenic *SK1* fragment from C57BL/6J and *Mus spretus* genomic DNA. The resulting amplimers were separated on a nondenaturing 0.5$\times$ mutation detection enhancement (MDE) (FMC) gel at 6 W for 20 hr. Amplimers were visualized by autoradiography because the SK16 primer had been end-labeled with ^{32}P before PCR amplification. A single-strand conformational polymorphism (SSCP) (21) was detected between C57BL/6J and *M. spretus*; this SSCP then was evaluated on the BSS backcross mapping panel available from the Jackson Laboratory (22). Offspring were scored as homozygous for the *spretus* allele or heterozygous for C57BL/6J and *spretus* alleles. Results were submitted to the Jackson Laboratory, where precise mapping was determined relative to previously tested markers.

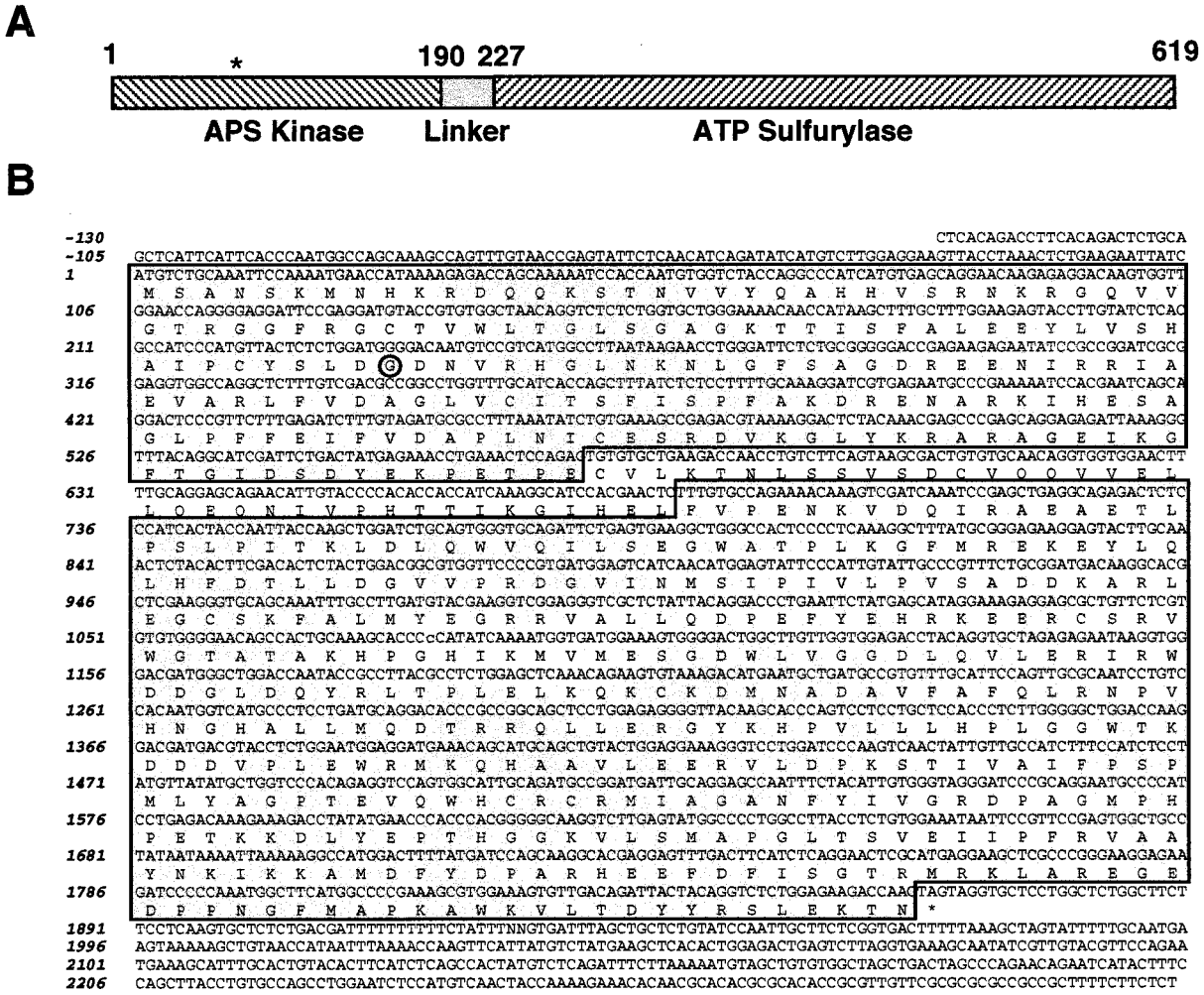

FIG. 2. Sequence of *SK2*. (*A*) Schematic diagram of ATP sulfurylase/APS kinase. Approximate location of the mutation in *bm SK2* is indicated by ∗. (*B*) The cDNA sequence and its deduced amino acid sequence are shown. The mutation found in *bm SK2* is circled.

Murine *SK2* was mapped by using the same approach, but with the murine *SK2*-specific primer pair SK12 (5′-GGAGAAAACCAACTAGGTGCTCCTGGC-3′) and SK13 (5′-CATAGTGGCTGAGATGAAGTGTACAGTGC-3′). This pair amplifies a 287-bp intragenic fragment of the *SK2* gene, which also has a single-strand conformational polymorphism between C57BL/6J and *M. spretus*. Offspring of the BSS backcross were scored for this *SK2* polymorphism and results were submitted to the Jackson Laboratory. *SK2* was found to cosegregate with *D19Mit13* (logarithm of odds 28.3 at $\theta = 0$) The human SK genes were placed on the genetic map via radiation hybrid mapping (23).

RESULTS

Cloning and Characterization of a *SK2* cDNA. The earlier cloning of the bifunctional murine SK (*SK1*) (11) did not identify the underlying etiology of the brachymorphic phenotype. Furthermore, we genetically mapped *SK1* to mouse chromosome 3, which is also incompatible with it being the cause of brachymorphism, which maps to chromosome 19 (12). These results led us to consider the possibility that more than one *SK* gene might be present in mice. A second *SK* isoform first was detected after sequence similarity searching (24, 25) using murine *SK1* as the query sequence. Two groups of murine ESTs were identified; one group having near identity to the query sequence and presumably representing *SK1* transcripts. The other group of ESTs had lower nucleotide homology, but high amino acid identity, and potentially represents novel *SK* isoforms. One of these latter ESTs was used to isolate the complete cDNA of an additional isoform,

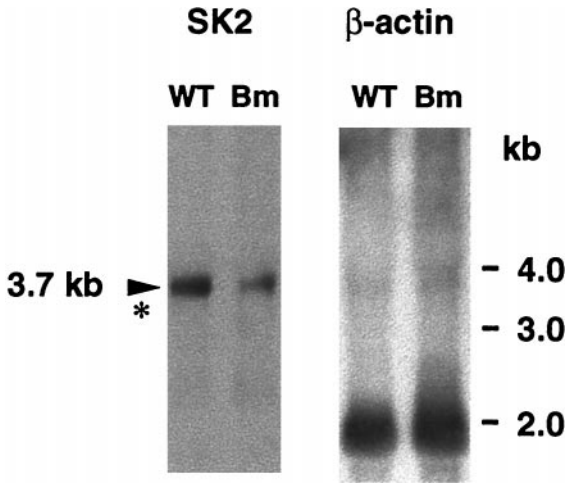

FIG. 3. Northern blot analysis of *SK2*. Fifteen micrograms of total RNA extracted from normal and brachymorphic liver was electrophoresed in a 1% agarose-formaldehyde gel and transferred to a Nytran filter. Hybridization with a ^{32}P-labeled 1.9-kb *SK2* cDNA yielded a single band at approximately 3.7 kb. Approximate location for the 3.3-kb *SK1* message is indicated by ∗. Hybridization with a mouse β-actin probe yielded a single band at approximately 1.8 kb.

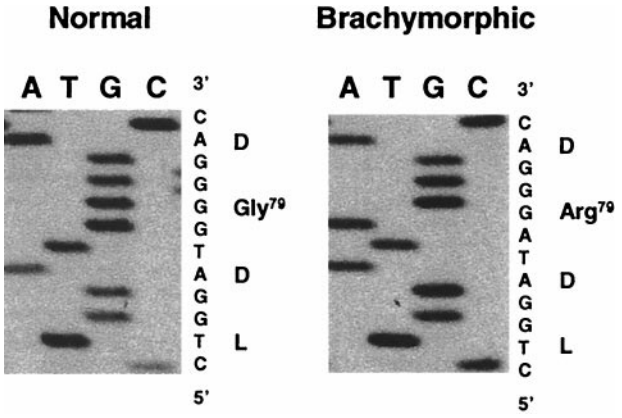

FIG. 4. Genomic DNA sequence at the mutation site from normal and *bm* mice. Position at nucleotide 235 is changed from G^{235} to A^{235} resulting in the amino acid change from Gly^{79} to Arg^{79} in the N-terminal APS kinase portion of the *bm* SK2.

referred to as *SK2*, from mouse total liver RNA by 5′-inverse PCR (20) (Fig. 2). *SK2* contains an uninterrupted coding sequence of 1,863 bp and has 76% identity at the amino acid level to SK1. SK2 also contains functional motifs previously associated with unifunctional ATP sulfurylases and APS kinases (11). Northern blot analysis reveals a single *SK2* transcript of 3.7 kb in normal and brachymorphic liver (Fig. 3), slightly larger than the 3.3-kb *SK1* transcript (11). The 3.7-kb *SK2* transcript also was detected in cartilage, skin, and brain (data not shown).

Chromosomal Localization of *SK1* and *SK2* Genes. *SK1* was found to cosegregate with *D3Xrf10*, a locus on the distal end of chromosome 3 (logarithm of odds 28.3 at $\theta = 0$), whereas *SK2* was mapped to chromosome 19 by using an intragenic single-strand conformational polymorphism on an interspecific backcross mapping panel. *SK2* is tightly linked to *D19Mit13*, as is the *bm* locus (19). Consequently, *SK2* was tested as a candidate for causing brachymorphism.

Mutation Analysis and Recombinant SK2 Enzyme Assays. Sequence analysis of wild-type and *bm SK2* cDNA revealed a single nucleotide change, a G to A transition, in the *bm* allele that changes a glycine residue to an arginine residue (Gly^{79} to Arg) in the APS-kinase domain of the bifunctional enzyme (Fig. 2). This change also is present in genomic DNA (Fig. 4). That the change causes disease is suggested by the conservation of this glycine residue in all previously characterized bifunctional SK proteins and in all unifunctional APS kinases (11). Further support for this mutation being the cause of the brachymorphic phenotype derives from *in vitro* assays of wild-type and mutant recombinant enzyme activities. Bacterially expressed recombinant SK2 protein was found to catalyze both ATP-sulfurylase and APS-kinase reactions, synthesizing PAPS comparably to SK1 (11). In contrast to recombinant expressed wild-type SK2, recombinant expressed SK2 protein containing the Gly^{79} to Arg mutation has no APS-kinase activity, although its ATP-sulfurylase activity is maintained (Fig. 5). Taken together these results indicate that this mutation is responsible for murine brachymorphism.

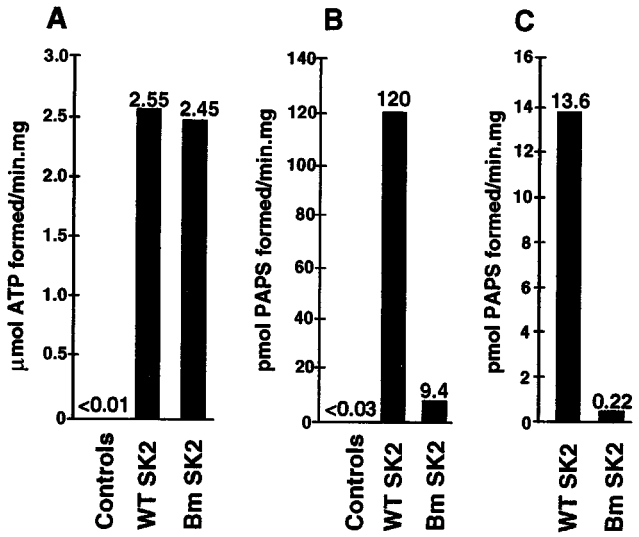

FIG. 5. Activities of the wild-type and brachymorphic SK2 enzyme. (*A*) ATP sulfurylase activity as measured by the reverse sulfurylase assay where formation of ATP is monitored. (*B*) APS kinase activity is measured as the amount of PAPS generated from APS and ATP. (*C*) PAPS synthetase activity is measured as the amount of PAPS generated starting from free sulfate and ATP. Controls in *A* and *B* represent DE3 cells and DE3 cells with pET-15b vector.

DISCUSSION

The activation of sulfate to produce the universal sulfate donor, PAPS, is critical to many processes, including the activation of numerous peptide and steroid hormones, the metabolism of catecholamines, the production of ceramide during brain development, the synthesis of sulfolipids in the reproductive system, the proper functioning of the blood coagulation cascade, the detoxification of endogenous compounds, and the modification of a variety of drugs, mutagens, and bile acids. Our results indicate a gene family is responsible for encoding this critical function and suggest nonredundant, tissue-specific role of each isoform, as demonstrated by the tissue-specific defect in PAPS synthesis in *bm* mice. Although the key steps in sulfating biomolecules have been assumed to be at the level of the myriad of sulfotransferases, our findings further demonstrate that regulation at the level of forming the sulfate donor is important as well, suggesting possible regulatory mechanisms at other steps along the overall sulfation pathway. Finally, the finding of additional ESTs (unpublished data), which have reduced nucleotide identity but high amino acid identity to SK1 and SK2, suggests that this family will likely grow.

It is intriguing that the *SK2* mutation specifically affects postnatal skeletal development and other selected tissues. Newborn *bm* mice appear skeletally normal, suggesting that the *SK2* gene product's principal role during skeletogenesis is during postnatal growth and that other SKs may substitute for SK2 *in utero*. It has been shown that hepatic detoxification in *bm* mice is principally via glucuronidation, whereas it is via sulfation in wild-type mice (26). Bleeding times are also abnormal in *bm* mice (19). However, other tissues that contain important sulfated biomolecules such as the kidney and brain appear normal in *bm* mice, suggesting tissue-specific sulfation mechanisms (17). Although the *SK2* transcript is found in total brain RNA, *bm* mice do not have an obvious neurologic phenotype. Careful neurological testing of *bm* homozygotes now is indicated to determine whether there may be subtle neurological effects, although absence of such a phenotype simply may represent functional redundancy for sulfate activation in the brain or a minor role for SK2 in this tissue. The contribution of each SK isoform during growth and development must await the identification of all family members and careful quantitation of their mRNA and protein levels. However, because it is now clear that the PAPS synthetases constitute a gene family, with known members lacking complete functional redundancy at the tissue level and with perhaps more members yet to be discovered, the *bm* mouse is an excellent model to study the role of sulfation in a variety of specific processes.

There are not yet human counterparts for the *bm* or other SK mutant phenotypes. Radiation hybrid mapping of the

human homologues of *SK1* and *SK2* place them on chromosomes 4q and 10q, respectively (unpublished data), consistent with the locations of other human genes whose mouse homologues are syntenic with the *SK* loci. At present no likely murine phenotype colocalizes with the *SK1* locus, nor have likely human phenotypes been mapped to regions containing the human *SK* homologues. However, human genetic disorders have been associated with mutations in other components of the sulfate metabolic pathway; for example, mutations at the locus encoding the high affinity sulfate transporter (DTDST), responsible for uptake of inorganic sulfate (one of the two substrates for SKs) into the cell, are associated with skeletal phenotypes also having undersulfated proteoglycans (27–29). Consequently, one would predict that mutations in *SK1* and *SK2* also will have consequences in humans.

We thank Lucy Rowe and Mary Barter for assistance in placing the *SK1* and *SK2* loci into the murine genetic map, Mary Lou Spach for maintenance of the brachymorphic colony, Judith Henry for tissue preparations, Glenn Burrell for manuscript preparation, and James Mensch for manuscript review. This work was supported by grants from the National Institute of Child Health and Human Development, the National Institute of Arthritis and Musculoskeletal and Skin Diseases, the Mitzutani Foundation, and the March of Dimes Foundation.

1. Schwartz, N. B., Lyle, S., Ozeran, J. D., Li, H., Deyrup, A., Ng, K. & Westley, J. (1998) *Chem. Biol. Interact.* **109,** 143–151.
2. Korch, C., Mountain, H. A. & Bystrom, A. S. (1991) *Mol. Gen. Genet.* **229,** 96–108.
3. Leyh, T. S., Vogt, T. F. & Suo, Y. (1992) *J. Biol. Chem.* **267,** 10405–10410.
4. Jain, A. & Leustek, T. (1994) *Plant Physiol.* **105,** 771–772.
5. Schwedock, J. S., Liu, C., Leyh, T. S. & Long, S. R. (1994) *J. Bacteriol.* **176,** 7055–7064.
6. Lyle, S., Stanzak, J., Ng, K. & Schwartz, N. B. (1994) *Biochemistry* **33,** 5920–5925.
7. Geller, D., Henry, J. G., Belch, J. & Schwartz, N. B. (1987) *J. Biol. Chem.* **262,** 7374–7382.
8. Lyle, S., Geller, D. H., Ng, K., Stanzak, J., Westley, J. & Schwartz, N. B. (1994) *Biochem. J.* **301,** 355–359.
9. Lyle, S., Ozeran, J. D., Stanzak, J., Westley, J. & Schwartz, N. B. (1994) *Biochemistry* **33,** 6822–6827.
10. Lyle, S., Stanzak, J., Westley, J. & Schwartz, N. B. (1995) *Biochemistry* **34,** 940–945.
11. Li, H., Deyrup, A., Mensch, J., Domowicz, M., Konstantinidis, A. & Schwartz, N. B. (1995) *J. Biol. Chem.* **270,** 29453–29459.
12. Lane, P. W. & Dickie, M. M. (1968) *J. Hered.* **65,** 297–300.
13. Schwartz, N. B. & Domowicz, M. (1998) *Am. Assoc. Orthoped. Surg. Publ.*, in press.
14. Schwartz, N. B., Ostrowski, V., Brown, K. S. & Pratt, R. (1978) *Biochem. Biophys. Res. Commun.* **82,** 173–178.
15. Sugahara, K. & Schwartz, N. B. (1979) *Proc. Natl. Acad. Sci. USA* **76,** 6615–6618.
16. Sugahara, K. & Schwartz, N. B. (1982) *Arch. Biochem. Biophys.* **214,** 589–601.
17. Sugahara, K. & Schwartz, N. B. (1982) *Arch. Biochem. Biophys.* **214,** 601–609.
18. Orkin, R. W., Williams, B. R., Cranley, R. E., Poppke, D. C. & Brown, K. S. (1977) *J. Cell Biol.* **73,** 287–299.
19. Rusiniak, M. E., O'Brien, E. P., Novak, E. K., Barone, S. M., McGarry, M. P., Reddington, M. & Swank, R. T. (1996) *Mamm. Genome* **7,** 98–102.
20. Zeiner, M. & Gehring, U. (1994) *BioTechniques* **17,** 1051–1053.
21. Orita, M., Iwahana, H., Kanazawa, H., Hayashi, K. & Sekiya, T. (1989) *Proc. Natl. Acad. Sci. USA* **86,** 2766–2770.
22. Rowe, L. B., Nadeau, J. H., Turner, R., Frankel, W. N., Letts, V. A., Eppig, J. T., Ko, M. S. H., Thurston, S. J. & Birkenmeier, E. H. (1994) *Mamm. Genome* **5,** 253–274.
23. Cox, D. R. (1992) *Cytogenet. Cell Genet.* **59,** 80–81.
24. Altschul, S. F., Gish, W., Miller, W., Myers, E. W. & Lipman, D. J. (1990) *J. Mol. Biol.* **215,** 403–410.
25. Boguski, M. S., Lowe, T. M. & Tolstoshev, C. M. (1993) *Nat. Genet.* **4,** 332–333.
26. Schwartz, N. B. (1983) in *Limb Development and Regeneration*, eds. Kelley, R. O., Goetinck, P. F. & MacCabe, J. A. (Liss, New York), Part B, pp. 97–103.
27. Hastbacka, J., Chapelle, A. d. l., Mahtani, M. M., Clines, G., Reeve-Daly, M. P., Hamilton, B. A., Kusumi, K., Trivedi, B., Weaver, A., Coloma, A., *et al.* (1994) *Cell* **78,** 1073–1078.
28. Hastbacka, J., Wilcox, W. R., Superti-Furga, A., Rimoin, D. L., Cohn, D. H. & Lander, E. S. (1996) *Am. J. Hum. Genet.* **58,** 255–262.
29. Superti-Furga, A., Hastbacka, J., Wilcox, W. R., Cohn, D. H., van der Harten, H. J., Rossi, A., Blau, N., Rimoin, D. L., Steinmann, B., Lander, E. S., *et al.* (1996) *Nat. Genet.* **12,** 100–102.